ECI 8th International Conference on Boiling and Condensation Heat Transfer
Ecole Polytechnique Fédérale de Lausanne, 3-7 June 2012
Lausanne, Switzerland

HEAT TRANSFER DURING THE CONDENSATION OF R134A INSIDE EIGHT PARALLEL MICROCHANNELS

Gil Goss Júnior and Júlio César Passos*
*Author for correspondence
LEPTEN/Boiling, Department of Mechanical Engineering
Federal University of Santa Catarina
Florianopolis-SC, Brazil, 88040-900
E-mail: jpassos@emc.ufsc.br

ABSTRACT

In this study the local heat transfer coefficient was investigated experimentally during the convective condensation of R-134a inside eight round (diameter D= 0.77 mm) horizontal and parallel microchannels. The test conditions included: $0.55 < x_v < 1$; $7.3 < p < 9.7$ bar; $17 < q'' < 53$ kW.m^{-2}; and $230 < G < 445$ kg.m^{-2}s^{-1}. The influence of temperature, heat flux, mass velocity and quality on the heat transfer coefficient, h, was evaluated. The results show that mass velocity and vapour quality have an important influence on the heat transfer coefficient. The consideration that all of the resistance to heat transfer is due to the conduction through the liquid film is a good approximation, mainly for $x_v < 0.95$. The experimental results were comparable with correlations and semi-empirical models described in the literature.

INTRODUCTION

The need to decrease both electricity consumption and CO_2 emissions has led to a growing interest in studies on microchannel condensation in the past decade. The goal of these studies is to increase the effectiveness of heat exchangers, due to the use of more compact systems, and to reduce the cost of materials and the quantity of refrigerant fluids used. One consequence of the miniaturization of condensers in air-cooled refrigeration systems, for example, is an increase in the COP caused by a decrease in the pressure drop on the air side, and an increase in the heat transfer coefficient on the refrigerant side. However, it can also lead to an increase in the pressure drop in the refrigerant flow.

Microcondensers are already used in several cooling and refrigeration processes, such as mini heat pipes and compact heat exchangers in the electronics industry, for thermal control in satellites, and in compact air conditioning - both residential and automotive. The latter has been making use of microchannels with hydraulic diameter, D_h, over the interval 0.5 mm < D_h< 1.5mm for nearly 20 years.

Complete overviews on microchannel condensation, for instance, Garimella (2006) and Ghiaasiaan (2008), have been published. However, we are still a long way from understanding the phenomena involving phase change in microgeometries, and thus the design of compact heat exchangers still represents a considerable challenge to industry. This is evidenced by the different results obtained by authors for the heat transfer and pressure drop.

As reported in Agarwal et al. (2010), Cavallini et al. (2006), Kim et al. (2003), Médéric et al. (2006), and Wang et al. (2002), for the heat transfer phenomena, the formulations developed for conventional channels do not work with the same precision in microchannels. The same applies to flow patterns, where the transitions differ for micro and macrochannel condensation (Agarwal et al. (2010), Wang et al. (2002), Coleman and Garimella (2000; 2003), Serizawa et al. (2002), Wang and Rose (2006)). These differences between macro and microchannels occur because of the different influences of the forces during the flow.

In microscale, the shear and surface tension forces are more important than the gravitational ones, and the opposite occurs when the diameter is larger, as reported in Agarwal et al. (2010), Cavallini et al. (2006),Wang et al. (2002), Coleman and Garimella (1999 ; 2000), Koyama et al. (2003), and Matkovic et al. (2009). Wang and Rose (2011) also cited another important effect in non-circular microchannel condensation: the viscosity in transverse flow.

Most of the correlations proposed to predict the pressure drop during condensation in microchannels are based on modifications from the Lockhart and Martinelli (1949), Chisholm (1973) and Friedel (1979) correlations, which were proposed for conventional diameters, and their results show large deviations compared with the experimental data of Dalkilic and Wongwises (2009).

In addition, the vast majority of the models developed for annular film condensation do not consider the interfacial resistance. Heat transfer in annular film condensation may be subject to additional intermolecular forces if the thickness is very small. We can consider here two important intermolecular effects that can occur at the interface of the condensation film: the

interface mass transfer (also called interfacial resistance) and the pressure jump. The latter is composed of two portions: disjoining and capillary pressure.

The interfacial resistance causes a temperature drop at the interface between the liquid and vapor, when there is a phase change. When the phase change rate is high, this effect can be important. As reported by Tanasawa (1991), this effect cannot be neglected in metal vapor condensation. According to Wang and Rose (2004), this effect is stronger only at low pressure, due to a low vapor density. As shown in Wang and Rose (2004), the interfacial resistance can be calculated as follows:

$$R_i = \frac{1}{4\zeta}\frac{(\gamma+1)}{(\gamma-1)}\frac{T_{Sat}\sqrt{R_{spec}T_{Sat}}}{\rho_l H_{lv}^2} \tag{1}$$

where T_{sat}, R_{spec}, ρ_l and H_{lv}, γ are the saturation temperature, the specific gas constant, the liquid density , the specific enthalpy of vaporization and the ratio between the principal specific heat capacities of the vapor, respectively. Besides, $\zeta = 0.665 \pm 0.003$.

The capillary pressure effect is based on the Young-Laplace equation, and it is present at any interface between two immiscible fluids. The strength of this effect varies according to the wettability and the surface tension of the fluids and is strong when the interface radius is small and for fluids with high contact angles, as in dropwise condensation. In channels this effect is important only when there is a corner in the cross section.

The disjoining pressure effect is a result of Van der Waals forces and it acts when two interfaces are very close to one another, one being influenced by the presence of the other. It is present in the process of condensation over a surface (solid-liquid and liquid-vapor interfaces). Here the liquid film thickness is, once again, a very important parameter. Wang et al. (2007) studied evaporation in a microchannel and found that capillary pressure plays an important role in the low liquid superheat phenomenon.

As reported in Nebuloni and Thome (2010), the disjoining pressure effect, for wetting fluids, can be calculated as a net mass flux per unit surface area where condensation to the liquid-vapor interface occurs, J_P:

$$J_P = \frac{2\rho_v}{\rho_l\sqrt{2\pi R_{spec}T_{Sat}}}\frac{C_H}{\delta^3} \tag{2}$$

Where T_{sat}, R_{spec}, ρ_l, ρ_v , δ and C_H are the saturation temperature, the specific gas constant, the liquid and vapor density, the liquid film thickness and the Hamaker constant (assumed to be equal to $2x10^{12}$ as suggested by Chien and Webb, 1998), respectively.

Based on this equation we can estimate a heat transfer resistance caused by the disjoining pressure effect, R_{dp}:

$$R_{dP} = \frac{1}{J_P H_{lv}} \tag{3}$$

where H_{lv} is the specific heat of vaporization.

Nebuloni and Thome (2010) developed a model to calculate the heat transfer coefficient for arbitrary channel geometries in the annular film condensation regime. This model includes surface tension, interfacial resistance, disjoining pressure and liquid-vapor mass transfer effects. It is associated with an average error of 11% in the h value, as obtained in several different experimental studies. These authors found that the interface effects are locally important where the film thickness is very thin, while the pressure jump effect does not play an important role within a diameter range of 0.54 - 1.1 mm. In addition, an enhancement of approximately 40% in the heat transfer was observed on decreasing the tube diameter from 1.1 mm to 0.54 mm.

Coleman and Garimella (1999; 2000) performed several experiments on flow visualization for adiabatic air-water flow and R-134a condensing in square horizontal microchannels with 1 mm < D_h < 4.91 mm. They observed that the hydraulic diameter has a substantial effect on the flow patterns and transitions. However, the tube shape had only a slight influence on the flow pattern. The same authors proposed different condensation flow regime maps for the diameter range studied. For G >150 kg.m^{-2}s^{-1}, they observed annular, wavy, intermittent (slug, plug) and dispersed flow. As D_h decreases, the annular regime is enhanced, and the area in the wavy regime decreases. For 1-mm tubes, the wavy regime completely disappears, confirming that the gravitational force diminishes in microchannels.

The wide applicability of microcondensers combined with the relative lack of knowledge on the phenomena occurring in microgeometries and the relatively weak prediction capacity in terms of flow behavior, leads to a need to perform new studies on the convective condensation in microchannels, mainly in submillimeter geometries, since most studies in this area are based on D_h > 1 mm, Garimella (2006).

The objective of this study was to analyze the convective condensation inside eight circular parallel and horizontal microchannels, with 0.77 mm of diameter. The test conditions were: $0.55 < x_v < 1$; $7.3 < p < 9.7$ bar; $17 < q'' < 53$ kW.,m^{-2} and $230 < G < 445$ kg.m^{-2}s^{-1}. The experimental data for the heat transfer coefficient are compared with four correlations proposed in the literature.

EXPERIMENT

Experimental facilities

Figure 1 shows the R-134a convective condensation loop installed in the LEPTEN laboratory at the Federal University of Santa Catarina, in Florianopolis, Brazil. The rig operates by producing R-134a vapor in the boiler and channeling it to the test section where different measurements are made. The working fluid is then turned into a liquid in a post condenser and pumped back to the boiler, as shown in Figure 1.

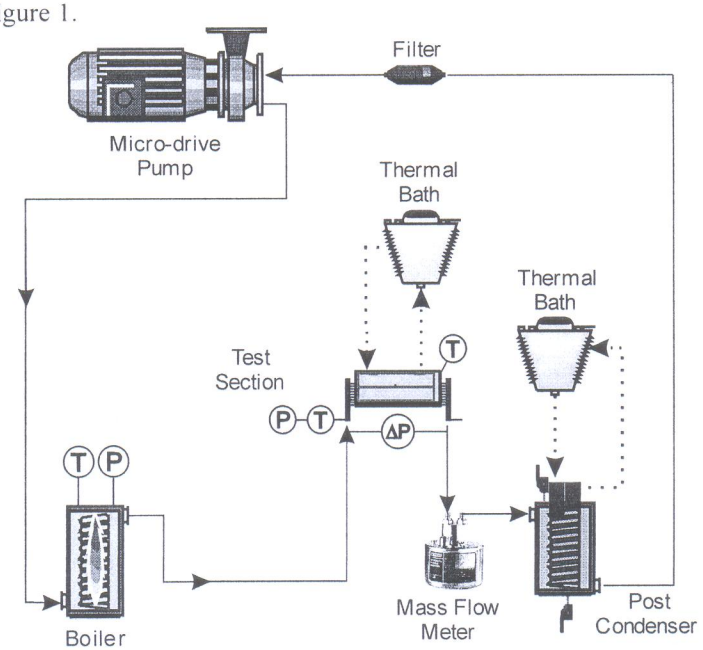

Figure 1 Scheme of experimental setup.

In the boiler, the temperature and pressure are measured, respectively, by an E-type thermocouple (Omega) and a pressure transducer (Wärme). A cartridge-type electrical resistance can be set to deliver power of up to 1000 W to the working fluid, depending on the mass flow required for the test, making it flow through a unidirectional valve to a superheater. The R-134a is heated to generate vapor with a few tenths of a degree of superheating. This happens because the resistance is installed in the top part of the boiler close to the outlet. The amount of liquid inside the boiler is monitored by a float and when the level is low a sensor triggers the pump, supplying R-134a.

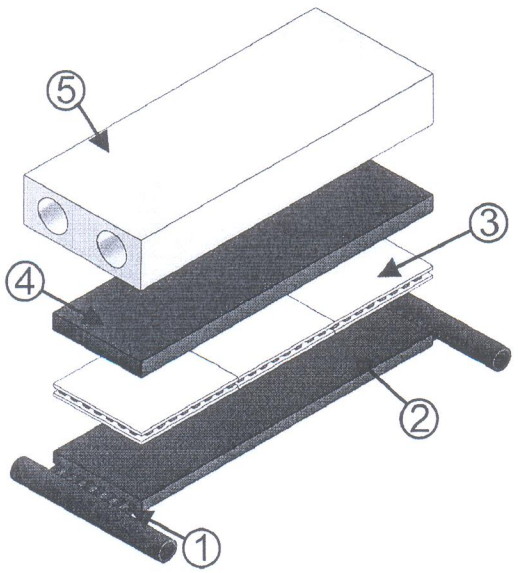

Figure 2 Test section exploded view.

The vapor reaches the test section, first arriving at a manifold, and then flows inside eight copper microchannels with D = 0.77 mm each and with 105 mm of length, as shown in (1) in Figure 2. The channels are assembled on a copper plate (2), with 3 mm of thickness and 90 mm of length, cooled by 3 Peltier coolers (by Danvic) placed above it (3). Each cooler has 30 x 30 mm^2 and both a cold and a hot side. The rig was assembled in such a way that the cold side is in contact with the copper plate (4), and the hot side is cooled by an aluminum heat sink (5) through which an ethylene-glycol and water mixture flows.

The pressure is measured by absolute (at the inlet manifold) and differential (between two manifolds) pressure transducers. The temperature is measured by thermocouples at both the entrance and exit manifolds, as well as at 13 different points on the copper plate, as shown in Figure 3. Unlike the other thermocouples, the one located at the center of the plate is not used to calculate the local heat transfer coefficient. It is used only to calculate the heat flux removed by the Peltier cooler, which is explained below.

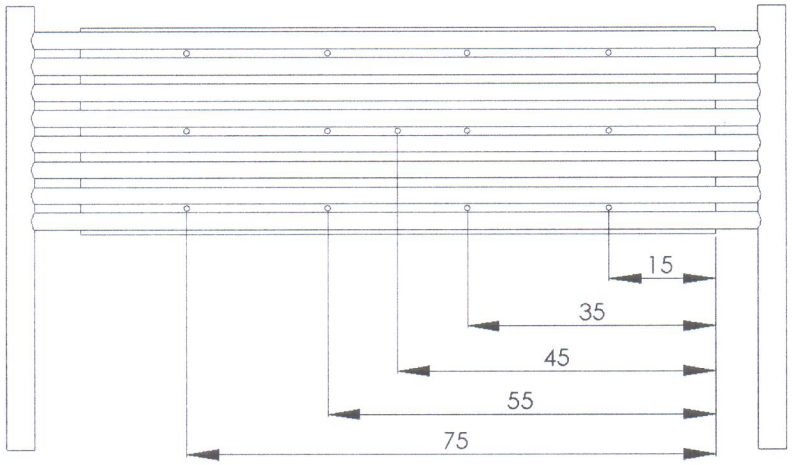

Figure 3 Location of the thermocouples in the test section (in mm).

A mixture of vapor and liquid leaves the test section, passes through a Coriolis mass flow meter (Siemens) and reaches a post condenser, which uses water from a thermal bath to totally condense the working fluid and adjust the pressure and flow velocity of the working fluid, as shown in Figure 1. The flow then reaches a filter to remove small particles and avoid problems occurring in the pump. The micropump is magnetically driven (Liquiflo), and operates with a maximum flow rate of 2 l/min and sends the R-134a back to the boiler when the level is low.

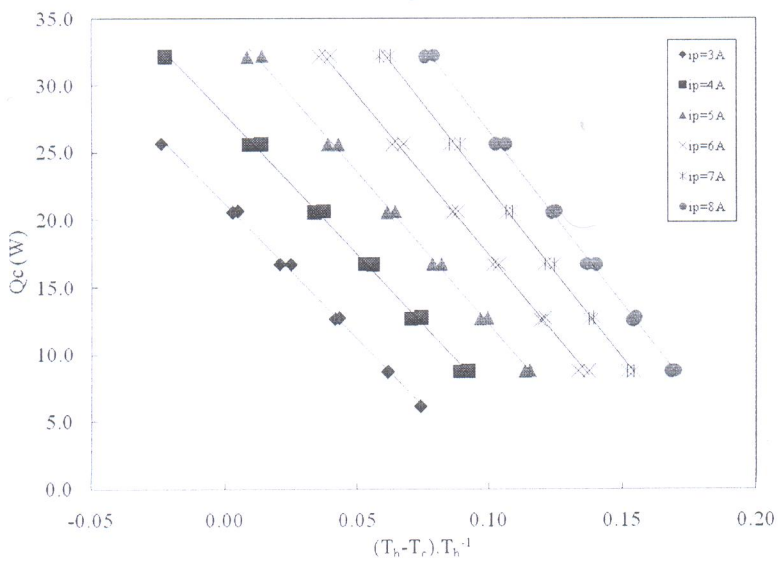

Figure 4 Calibration curves of Peltier cooler.

Each of the three Peltiers is calibrated to allow the calculation of the heat flux removed from the fluid. The power removed (Qc) was found to be a function of the electrical current supplied (ip) and the temperatures on the cold (T_c) and the hot side (T_h) sides of the coolers. This calibration procedure had an uncertainty of 1 W (with 95% confidence) for the heat removed. Figure 4 shows the curves for one Peltier cooler.

Data reduction

From the temperature measured at the inlet and outlet of the test section and over the copper plate, the pressure measured at the inlet and outlet of the test section, the mass flow rate and the heat flux, we can define the flow conditions over the test section length, and calculate the heat transfer coefficient at the points where the wall temperature is measured.

The first step is to determine the location where the two-phase flow starts, because vapor at the entrance manifold is superheated. From the temperature and pressure measured at the entrance of the test section, and with the heat flux removed, the average temperature of the fluid in a microchannel (with a heat balance) and the pressure (using the Blasius pressure drop

correlation) at each position can be calculated. The location where the two-phase starts is where the saturation pressure based on the temperature and the pressure calculated using a pressure drop correlation are equal.

With this position determined, the pressure drop is assumed to be linear from this location up to the end of test section. Thus, the pressure at each location of the test section can then be determined. The calculations are carried out using the mean mass velocity, defined as the total mass velocity divided by the number of channels (eight). This assumption considers that the flow is homogeneously distributed. As reported by Vist and Pettersen (2004), this is a good approximation, because the flow condition at the entrance is in the vapor phase.

The enthalpy at the desired location is determined by a heat balance, using the heat flux removed by the Peltier coolers. Since the local enthalpy is determined, the quality can be calculated using this value and the pressure (which is linearized). The experimental local convective condensation heat transfer coefficient, h, is defined as:

$$h_{exp} = \frac{q''}{T_{Sat} - T_w} \tag{4}$$

where q'', T_{sat} and T_w represent the heat flux, the local saturation temperature and the wall temperature, respectively.

The heat flux is measured by the Peltier coolers, based on the characteristic curves obtained experimentally, which are shown in Figure 4. The local saturation temperature is a function of the local pressure, which is determined by linear interpolation. The wall temperature is experimentally determined from the average of the three readings taken at a particular location, shown in Figure 3.

Uncertainty analysis

The analysis of the uncertainties for the present experimental parameters determined according to Holman (1989) are summarized in Table 1. Figure 5 shows the uncertainty for the heat transfer coefficient as a function of the quality.

Table 1 Experimental heat transfer coefficient uncertainty.

Parameter	Uncertainty
Tube diameter, d	±1.5%
Surface Area, A	±2.0%
Wall temperature, T_w	±0.3 K
Fluid temperature, T_f	±0.5 K
Pressure, p	±5 kPa
Pressure drop, Δp	±0.75 kPa
Mass velocity, G	±5%
Heat flux, q''	±3%
Experimental heat transfer coefficient, h	see Figure 5

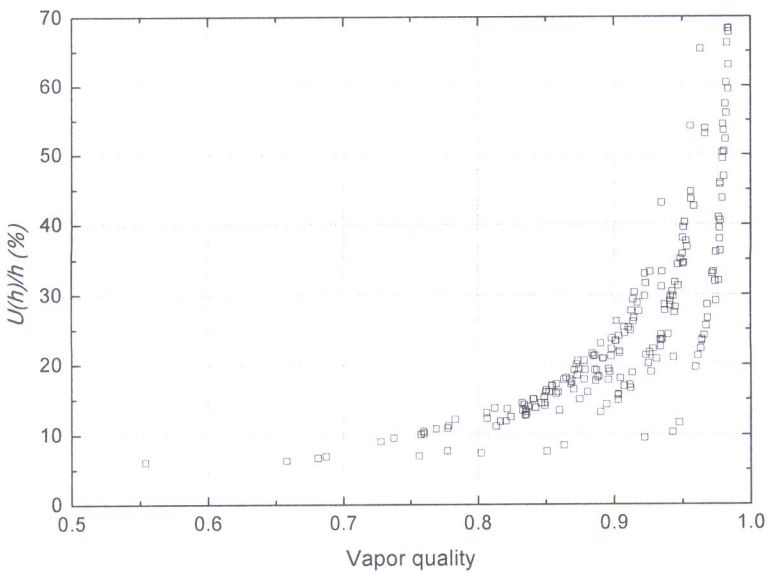

Figure 5 Relative uncertainty for the h as a function of the vapor quality.

RESULTS

Figure 6 presents all data points plotted on the Coleman and Garimella (2000) map. According to this map, it can be seen that all points are in the annular and mist flow regimes.

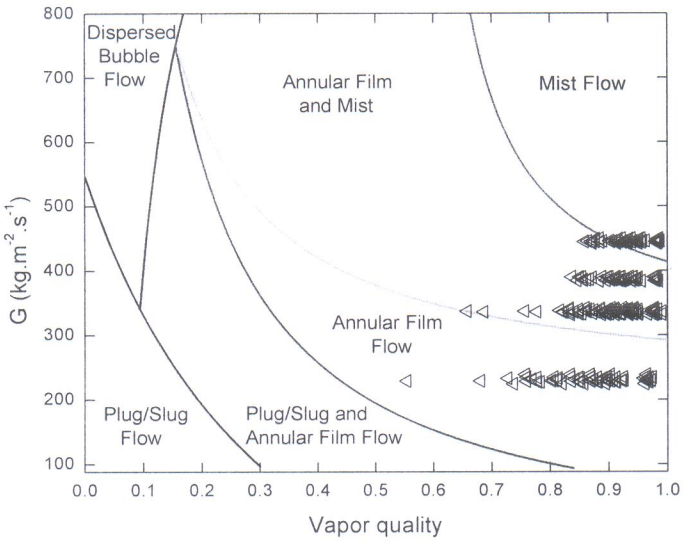

Figure 6 Experimental data points on the Coleman and Garimella (2000) map.

In the next sections, the influence of some parameters on the experimental results for the heat transfer coefficient and the comparison of the experimental results with some correlations will be presented and discussed.

Effect of mass velocity

Figure 7 shows that the heat transfer coefficient always increases with the mass velocity under the measured conditions. This effect is even strong for higher vapor qualities and mass velocities ($G > 335$ kg.m^{-2}s^{-1}). This result shows that the shear stress at the liquid-vapor interface is an important force in the flow. This is characteristic of mist and annular flow patterns.

For the same quality and heat flux, an increase in the mass velocity implies a higher shear between the vapor and the liquid. This causes a thinning of the liquid film in the annular flow. Furthermore, for the mist flow the amount of entrainment liquid increases. These factors lead to a higher heat transfer coefficient in a condensation flow where the dominant heat transfer mechanism is conduction through the liquid film.

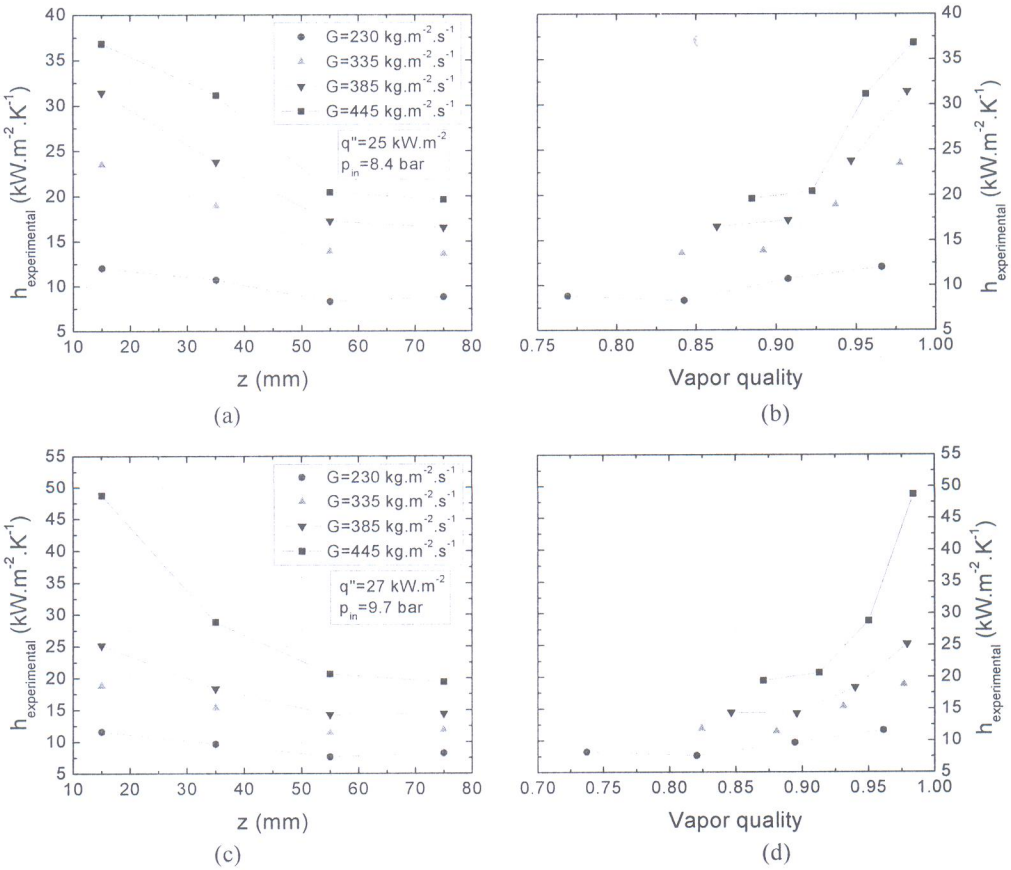

Figure 7 Mass velocity influence on the *h* value as a function of the position in the test section (a and c) and of the local quality (b and d) for different test conditions.

Effect of heat flux

The influence of the heat flux on the heat transfer coefficient is not clear for the present test conditions. As can be seen in Figure 8, the heat flux variation causes little difference in the heat transfer coefficient, mainly for higher qualities. For the test conditions showed in Figure 8, for $x_v < 0.9$ there is a tendency for the h to increase as the heat flux decreases. However, this difference is very small, sometimes being in the same order of magnitude as the experimental uncertainty.

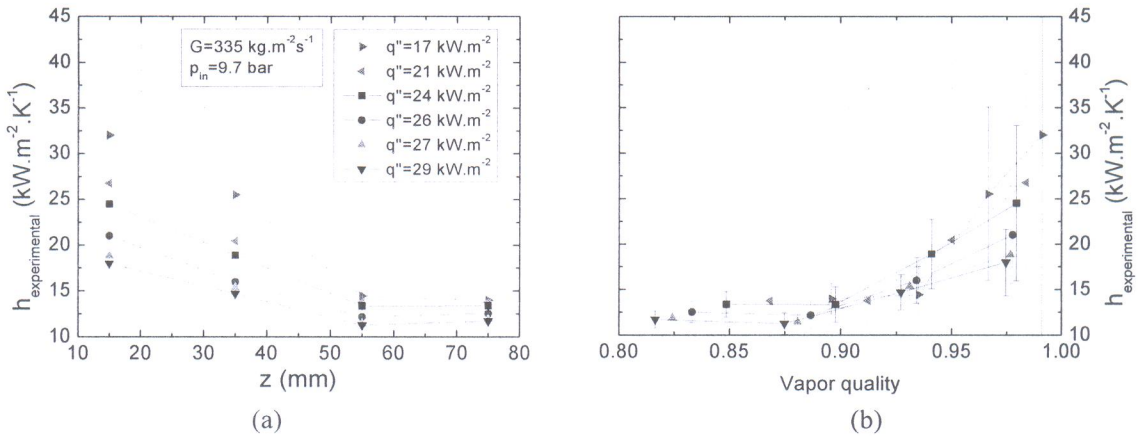

Figure 8 Mean heat flux influence on h as a function of: a) the location in the test section; and b) the local quality.

Effect of saturation temperature

As in the case of the heat flux, there is no effect of saturation temperature on the heat transfer coefficient for the conditions tested. Figure 9 shows the influence of the saturation temperature for two different heat flux and mass velocity conditions. For all of the different saturation pressures the difference in the heat transfer coefficient is less than the uncertainty.

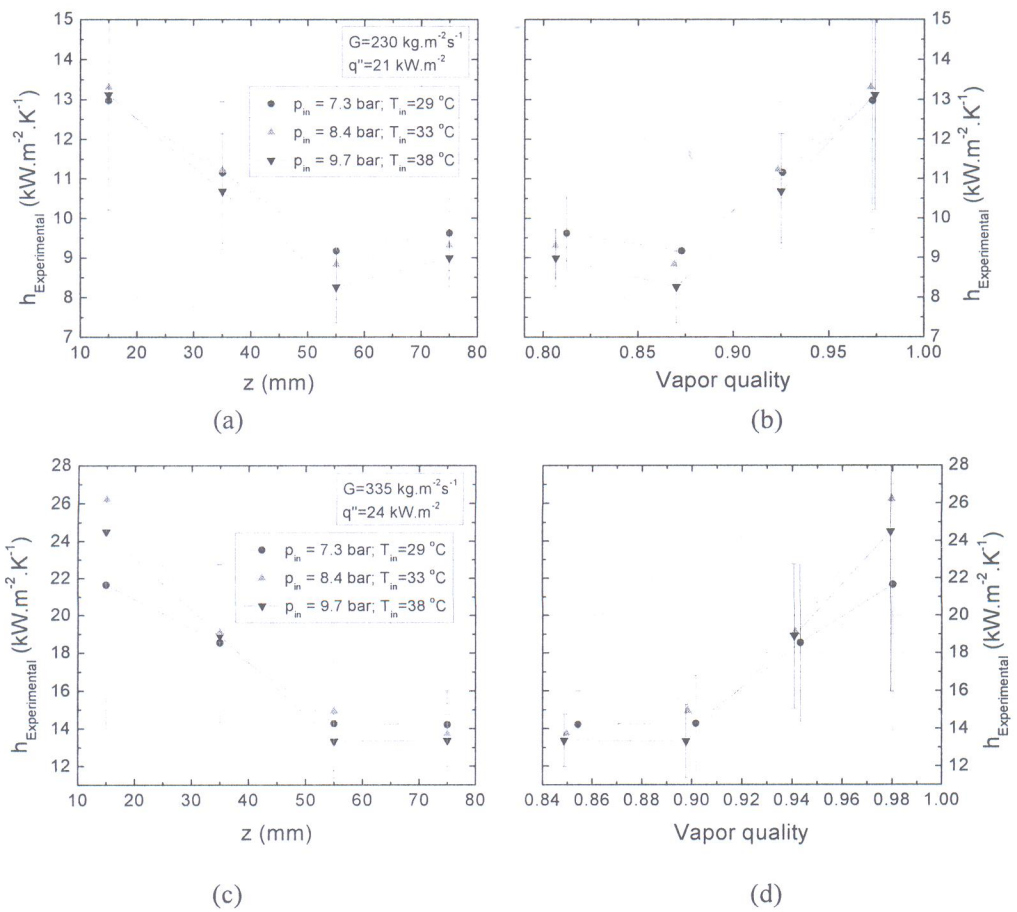

Figure 9 Saturation temperature/pressure influence on the h as a function of the position in the test section (a and c) and of the local quality (b and d) for different test conditions.

This is caused by a compensation effect between the condensate film properties and the flow characteristics. Increasing the fluid temperature can result in an increase in the heat transfer through the liquid film, because the liquid properties change (conductivity coefficient, density, etc.), causing an enhancement in the h. On the other hand, if the vapor temperature increases the vapor velocity decreases, reducing the interfacial shear stress between the liquid and the vapor.

Effect of vapor quality

We can note two different behaviors in Figure 10. Firstly, as expected for annular flow, the h decreases with reducing vapor quality, until a certain value, depending on the test conditions. This happens because, in this flow pattern, the thickness of the condensate is the dominant resistance in the heat transfer process. On reducing the quality, the quantity of the fluid and the thickness of the liquid film increases, raising the heat transfer resistance. According to this explanation, it is expected that the heat transfer coefficient continues to decrease.

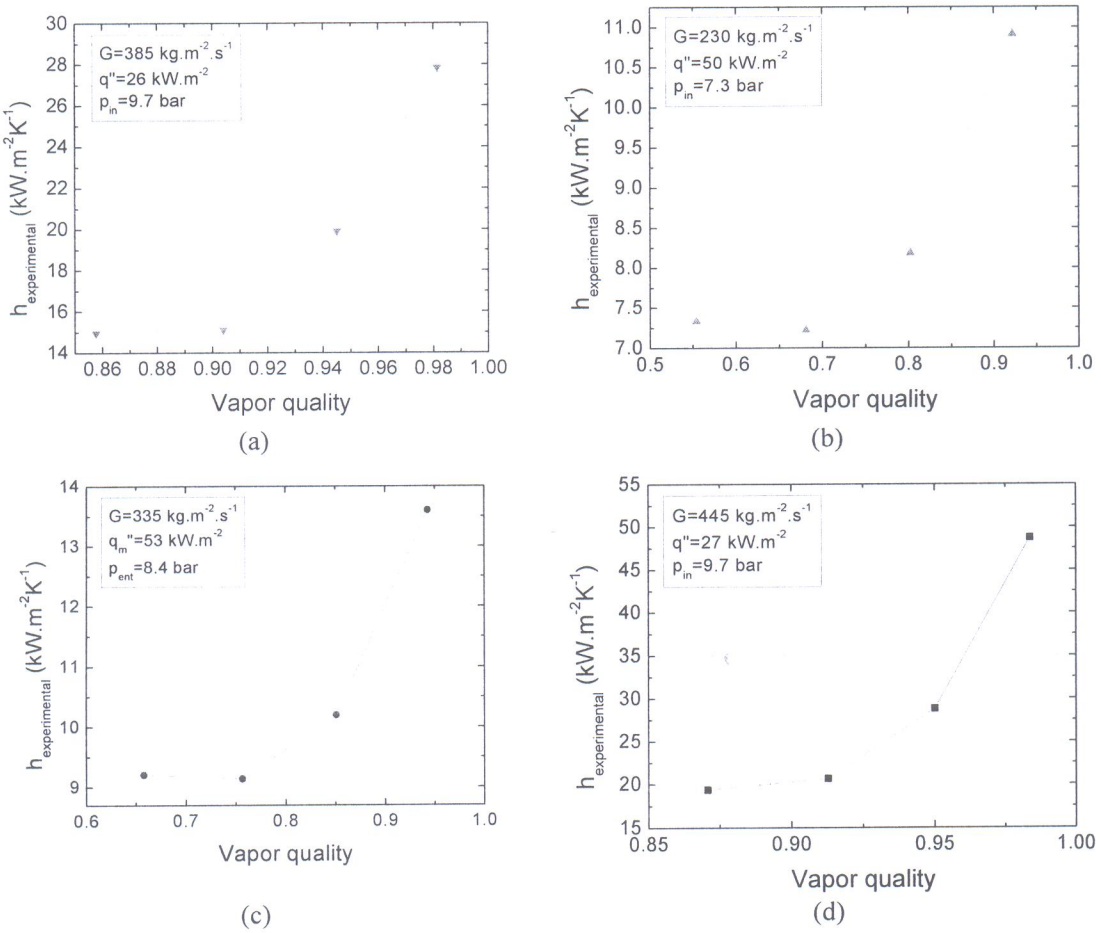

Figure 10 Influence of the vapor quality on heat transfer coefficient for different test conditions.

The second part, however, shows that with a decrease in the quality to below a certain value the heat transfer coefficient tends to be constant. At the beginning of the condensation the liquid film is very thin and probably covers the whole tube perimeter. In this situation, the surface tension and the shear forces are predominant over the gravity force. As the quality decreases the quantity of liquid increases and it tends to accumulate on the bottom of the tube. Thus, we can separate the heat transfer through the tube into two different parts: the top and the bottom.

Due to the difference between the density of the liquid and the vapor, with an increasing amount of liquid the vapor flows with reduced velocity, reducing the shear force. These characteristics contribute to a short stratification of the flow, causing a thicker film in the bottom compared with the top of the tube. The liquid accumulation causes a poor heat transfer region on the bottom of the tube. On the top of the tube, however, the liquid film continues to be thin, continuing to present high h values and compensating for the bottom part. For large tubes, these two regions are called active (top) and flooded or inactive (bottom) heat transfer regions. This stratification was also described in a numerical study developed by Wang and Rose (2006), for circular tubes with D = 1 mm.

Furthermore, a large decrease in the h value is noted for the first 5% of the quality reduction. There are two possible explanations for this, both related to the film thickness. One of them is that the liquid film is not completely formed, because the amount of liquid is too low. Thus, what occurs is the intermittent formation and suppression of this very thin liquid film. It is almost like droplet condensation, which increases the h value considerably. This hypothesis is not easy to prove, because the

visualization of this film is difficult. Also, a study carried out by Nebuloni and Thome (2010), for circular tubes with D = 1 mm, showed similar results, even considering that the liquid film was already formed at the entrance of the tube.

The second explanation is that the liquid film is too thin, and therefore the heat conduction resistance is not dominant in this region. Thus, other effects, such as interfacial resistance, disjoining pressure, liquid-vapor mass transfer and the boundary layer development may play important roles. In order to consider this problem, it is recommended that the apparent thickness of the liquid film is calculated from the experimental results, based on the assumption that the only heat transfer resistance is due to the heat conduction through the condensate, and the temperature profile over the film is linear. In this case we have:

$$\delta_{exp} = \frac{k_l}{h_{exp}} \tag{5}$$

where k_l and h_{exp} represent the liquid conductivity and the experimental heat transfer coefficient (Eq. 4), respectively.

If we consider that the liquid film has a uniform thickness without waves at the liquid-vapor interface, we can use the follow equation to calculate the film thickness:

$$\delta = \frac{D}{2}(1 - \sqrt{\alpha}) \tag{6}$$

where D and α represent the tube diameter and the void fraction, respectively.

Figure 11 shows a comparison between the value obtained with Eq. 5 and the film thickness calculated using Eq. 6 where the void fraction is determined by the correlation proposed by Graham (1998) and the homogeneous model. All the data predicted using the homogeneous model under predict the experimental points. That is expected, because this model normally fits well the data in the dispersed bubble flow region.

From Figure 11 we can conclude that the consideration that the heat conduction resistance is the only resistance to the heat transfer is very good for qualities below 0.95. Above this value, the δ values based on experimental data (using Eq. 5) are mostly higher than the values calculated using the Graham (1998) correlation. This means that there are other important heat transfer resistances contributing to this phenomenon. In other words, the thickness of the liquid film is so thin that other resistances play important roles, as reported previously.

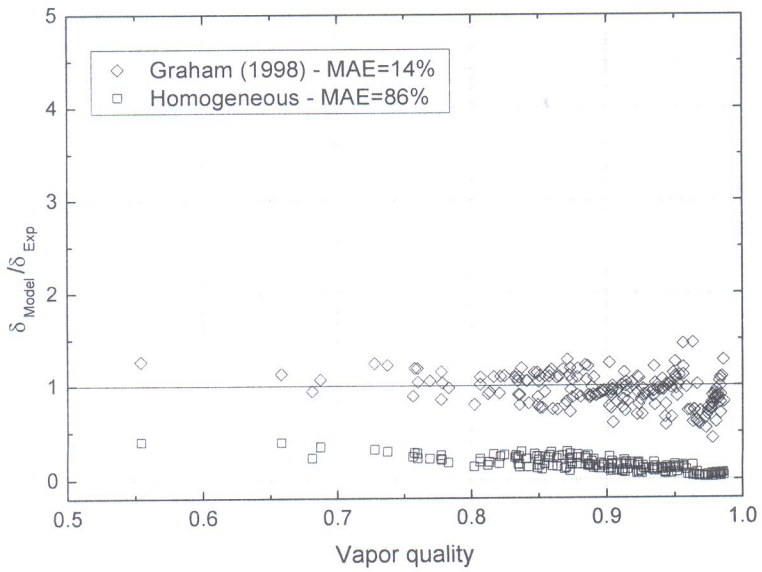

Figure 11 Comparison between δ values - experimental and theoretical (based on the Graham (1998) correlation for a void fraction).

To better analyze this behavior we can compare the values for the interfacial (Eq. 1), disjoining pressure (Eq. 3) and conduction resistance (Eq. 7):

$$R_{cond} = \frac{\delta_{exp}}{k_l} \tag{7}$$

where k_l and $\delta_{exp.}$ represent the thermal conductivity of the liquid and the film thickness. The latter is calculated using Eq. (5).

Figure 12 shows a comparison of these three types of resistances.

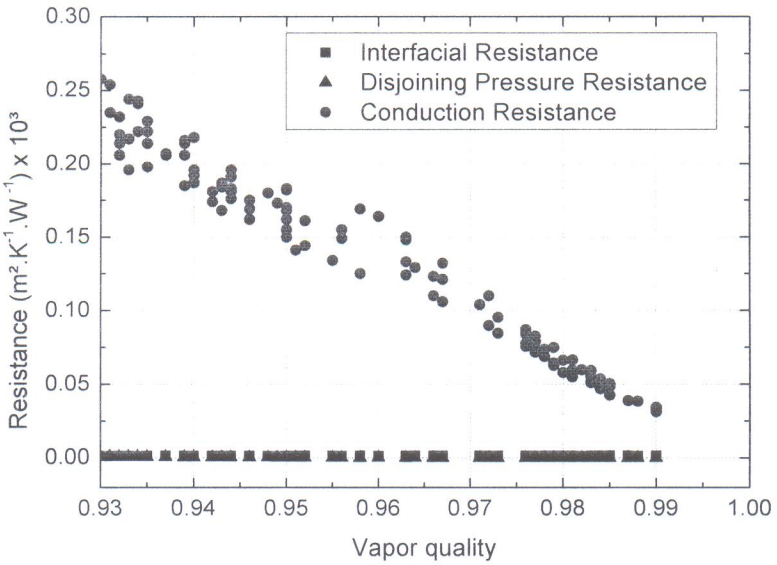

Figure 12 Comparison of the interfacial, disjoining pressure and conduction resistances for high vapor qualities.

Figure 12 shows that for all points the resistance due to heat conduction is higher than the other two sources. For very high qualities, where the values are closer, the conduction resistance is more than ten times higher than the disjoining pressure and the interfacial resistance. This means that another phenomenon occurring in this region may be responsible for this behavior. This may be connected to the presence of the wave in the film or even the axial conduction in the tubes, which are not considered in this study. As reported by Chiapero *et al.* (2011), for boiling heat transfer, the axial heat flux plays a very important role in the transition region (onset boiling). Similar behavior can be considered regarding the onset of convective condensation, in the region where the flow is predominantly single phase (that is, vapor with only a few liquid drops since the condensation has just begun).

Comparison of experimental heat transfer coefficient with correlations

The comparison of the experimental heat transfer coefficient values obtained in this study with those calculated using four correlations can be estimated through the mean absolute error (MAE), defined as follows:

$$MAE = \frac{1}{N}\sum_{1}^{N}\left|\frac{h_{experimental} - h_{predicted}}{h_{experimental}}\right| \tag{8}$$

where $h_{experimental}$ and $h_{predicted}$ represent the experimental value and that predicted from the correlation heat transfer coefficient and N represents the number of data points.

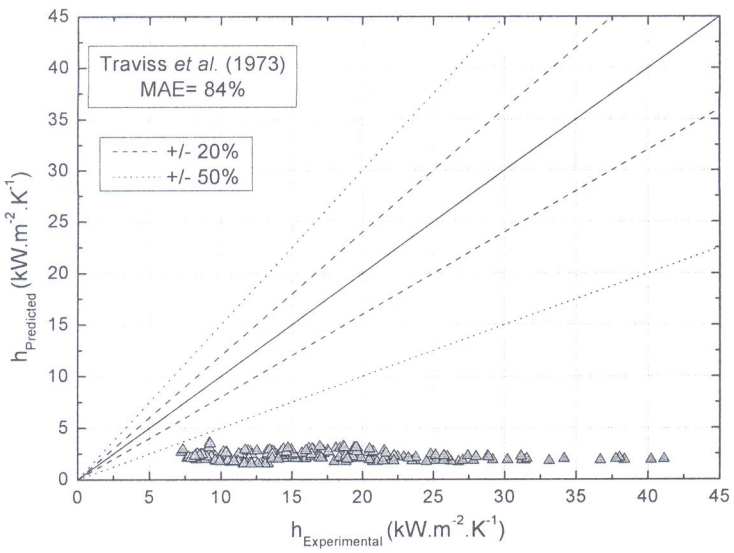

Figure 13 Comparison of the experimental heat transfer coefficient with the macro-channel correlation of Traviss *et al.* (1973).

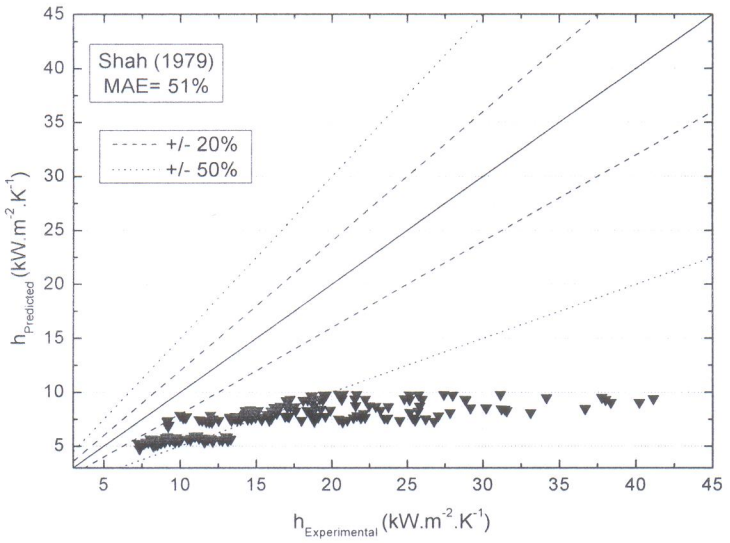

Figure 14 Comparison of the experimental heat transfer coefficient with the macrochannel correlation of Shah (1979).

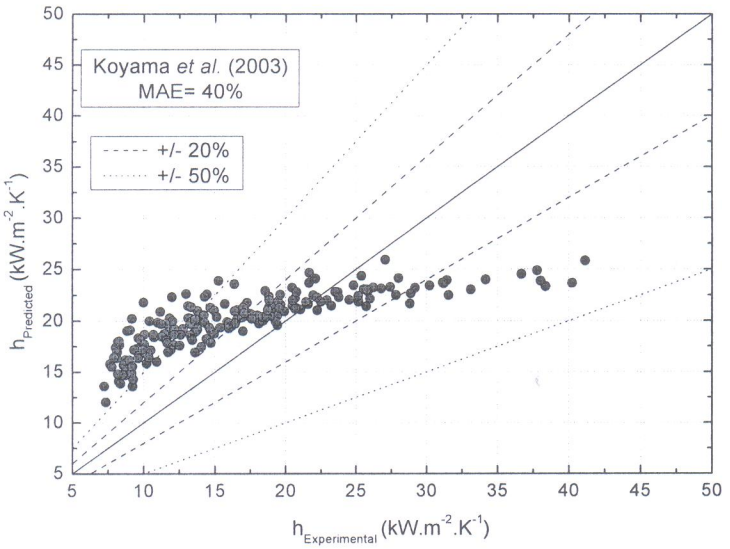

Figure 15 Comparison of the experimental heat transfer coefficient with the microchannel correlation of Koyama *et al.* (2003).

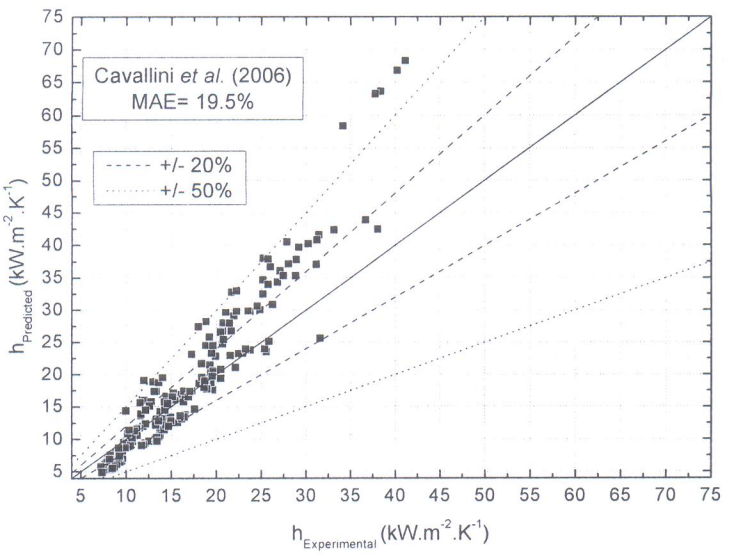

Figure 16 Comparison of the experimental heat transfer coefficient with the microchannel correlation of Cavallini *et al.* (2006).

Figures 13 to 16 present a comparison of the experimental results for the heat transfer coefficient with those predicted using the correlations of Traviss *et al.* (1973), Shah (1979), Koyama *et al.* (2003) and Cavallini *et al.* (2006). The first two were obtained to predict the heat transfer coefficient for conventional diameters, and the last two for condensation in microchannels.

It can be observed in Figures 13 and 14 that the tested correlations obtained for conventional (macro) channels do not adequately predict the experimental data. This behavior is discussed above and is a result observed by different authors for condensation in microchannels. The correlations of Traviss *et al.* (1968) and Shah (1979) presented MAE values of 84% and 51%, respectively, and thus these correlations underestimated the experimental data.

Based on the results described we can conclude that the correlation proposed by Cavallini *et al.* (2006) best fits the experimental results (Figure 16), presenting a MAE of 19.5%. This semi-empirical correlation was developed to predict the heat transfer coefficient in annular and annular mist flow regimes. The model takes into account the entrainment liquid in the mist flow. The quality of the correlation fit declines only for the highest h values, partly because of the high uncertainty at these points and partly due to the different mechanisms that can operate in this region, as discussed in the previous section.

The correlation of Koyama *et al.* (2003) presented an MAE of 40% compared with the experimental data. Although applied to refrigerant fluids in microchannels, it is not clear for which flow regimes this formulation was developed.

CONCLUSIONS

The experimental characteristics of the heat transfer coefficient were investigated for the condensation of R-134a inside eight parallel microchannels with D = 0.77 mm. The following conclusions can be drawn from this study.

There is no clear influence of the fluid saturation temperature and the heat flux removed on the heat transfer coefficient for the range tested. On the other hand the h increases with the mass velocity. The same occurs regarding the vapor quality, for high x_v.

For moderate qualities, the h tends to be constant, showing the influence of gravity, which leads to different liquid film thicknesses. For $x_v > 0.95$, the heat transfer coefficient reaches very high values.

It is demonstrated that the consideration that all of the heat transfer resistance is due to the heat conduction through the liquid film is a good approximation, mainly for $x_v < 0.95$. The interfacial and disjoining pressure resistances can be neglected even in the higher quality range. Further investigations should be carried out in order to better understand the condensation phenomena in the high vapor quality region.

The correlation proposed by Cavallini et al. (2006) for the heat transfer coefficient gave the best results compared with the experimental data. In contrast, the correlations tested which are proposed for conventional diameters gave the worse results, corroborating the fact that these formulations do not predict well the heat transfer in microchannels.

NOMENCLATURE

C_H	Hamaker constant ($=2 \times 10^{12}$)
D	diameter, m
G	mass velocity, $kg.m^{-2}s^{-1}$
h	heat transfer coefficient, $W.m^{-2}K^{-1}$
H_{lv}	specific enthalpy of vaporization, $J.kg^{-1}$
J_p	net mass flux in the liquid-vapor interface, $kg.m^{-2}.s^{-1}$
k	thermal conductivity coefficient, $W.m^{-1}K^{-1}$
MAE	mean absolute error, %
p	pressure, bar
R	thermal resistance, $m^2.K^{-1}.W^{-1}$
R_{spec}	specific gas constant ($=81.49$ $J.kg^{-1}K^{-1}$)
q''	heat flux, $W.m^{-2}$
T	temperature, K
x_v	vapor quality

Greek symbols:

α	void fraction
δ	liquid film thickness, m
γ	ratio of the principal specific heat capacities of the vapour
ρ	density, $kg.m^{-3}$
ς	constant ($= 0.665 \pm 0.003$)

Subscripts:

exp	experimental
cond	conduction
dp	disjoining pressure
i	interfacial
in	inlet
v	vapor phase
l	liquid phase
sat	saturation
w	wall

ACKNOWLEDGEMENTS

The authors gratefully acknowledge support of this work by Brazilian National Council of Research (CNPq), through the Universal Program. One of the authors, GGJ, thanks CNPq for providing a master of science scholarship. The authors wish to express their gratitude to Mr. Andre Manoel Oliveira and Mr. Stefano Macarini for their help with the laboratory work.

REFERENCES

Agarwal, A., Bandhauer, T. M., Garimella, S. (2010). Measurement and modeling of condensation heat transfer in non-circular microchannels, *International Journal of Refrigeration*, Vol. 33, pp. 1169 - 1179.

Cavallini, A., Doretti, L., Matkovic, M., Rossetto L. (2006). Update on condensation heat transfer and pressure drop inside minichannels, *Heat Transfer Engineering*, Vol. 27 pp. 74-87.

Coleman, J. W., and Garimella, S. (1999). Characterization of two- phase flow patterns in small diameter round and rectangular tubes, *International Journal of Heat and Mass Transfer*, Vol. 42, pp. 2869-2881.

Coleman, J.W., and Garimella, S. (2000), Two-phase flow regime transitions in microchannel tubes: The effect of hydraulic diameter, *ASME HTD*, Vol. 366 (4), pp. 71-83.

Coleman, J. W., Garimella, S. (2003) Two-phase flow regimes in round, square and rectangular tubes during condensation of refrigerant R134a, *International Journal of Refrigeration*, Vol. 26, pp. 117-128.

Chiapero, E. M., Fernandino, M., Dorao, C.A. (2011). Study of the influence of axial conduction in a boiling heated pipe, *Chemical Engineering Research and Design, (in press).*

Chien, L. H., Webb, R. L. (1998). A nucleate boiling model for structured enhanced surfaces, *International Journal of Heat and Mass Transfer*, Vol. 41, pp. 2183-2195.

Chisholm, D. (1973). Pressure gradients due to friction during the flow of evaporating two-phase mixtures in smooth tubes and channels, *International Journal of Heat and Mass Transfer*, Vol. 16, pp. 347–358.

Dalkilic A.S., and Wongwises S. (2009). Intensive literature review of condensation inside smooth and enhanced tubes, *International Journal of Heat and Mass Transfer*, Vol. 52, pp. 3409-3426.

Friedel, L. (1979) Improved frictional pressure drop correlations for horizontal and vertical two-phase pipe flow, i*n Eur. Two Phase Group Meeting, E2,* Ispra, Italy.

Garimella, S. (2006). Condensation in minichannels and microchannels, in: S. Kandlikar, S. Garimella, D. Li, S. Colin, M. R. King (Eds.), Heat transfer and fluid flow in minichannels and microchannels, *Elsevier Publications*, Oxford, UK, 1st edition.

Ghiaasiaan, S. M. (2008) Two-Phase Flow, Boiling, and Condensation, *Cambridge University Press*, New York, NY, 1st edition.

Graham, D. (1998). Experimental investigation of void fraction during refrigerant condensation, Master's thesis, Mechanical and Industrial Engineering Department, University of Illinois, Urbana, IL.

Holman, J. P. (1989). Experimental Methods for engineers, Mc Graw Hill, Singapore,

Kim, M. H., Shin, J. S., Huh, C., Kim, T. J., and Seo, K. W. (2003). A study of condensation heat transfer in a single mini-tube and review of korean micro- and mini-channel studies, *1st Int. Conf. on Microchannels and Minichannels*, Rochester, pp. 47–58.

Koyama, S., Kuwahara, K., Nakashita, K. Yamamoto, K. (2003). An experimental study on condensation of refrigerant R134a in a multi-port extruded tube, *International Journal of Refrigeration*, Vol. 24, pp. 425-432.

Lockhart, R.W., Martinelli, R.C. (1949). Proposed correlation of data for isothermal two-phase, two-component flow in pipes, *Chem. Eng. Prog.* pp. 39-48.

Matkovic, M., Cavallini, A., Del Col, D., and Rossetto, L. (2009). Experimental study on condensation heat transfer inside a single circular minichannel, *International Journal of Heat and Mass Transfer*, Vol. 52, pp. 2311-2323.

Médéric, B., Lavieille, P., Miscevic, M. (2006). Heat transfer analysis according to condensation flow structures in a minichannel, *Experimental Thermal and Fluid Science,* Vol. 30, pp. 785-793.

Nebuloni, S., Thome, J. R. (2010). Numerical modeling of laminar annular film condensation for different channel shapes, *International Journal of Heat and Mass Transfer*, Vol. 53, pp. 2615-2627.

Serizawa, A., Feng, Z., Kawara, Z. (2002). Two-phase flow in microchannels, *Experimental Thermal and Fluid Science*, Vol. 26, pp. 703- 714.

Shah, M. M. (1979). A general correlation for heat transfer during film condensation inside pipes, *International Journal of Heat and Mass Transfer*, Vol. 22, pp. 547-556.

Tanasawa, I. (1991). Advances in condensation heat transfer, in: J. P. Hartnett, T. F. I. Jr., Y. I. Cho (Eds.), Advances in Heat Transfer, Vol. 21, Elsevier, pp.55-139.

Traviss, D.P., Rohsenow, W.M., Baron, A.B. (1973). Forced-convection condensation inside tubes: a heat transfer equation for condenser design, *ASHRAE Trans.*, Vol. 79, pp. 157–165.

Vist, S., Pettersen, J. (2004). Two-phase flow distribution in compact heat exchanger manifolds, *Experimental Thermal and Fluid Science*, Vol. 28, pp. 209- 215.

Wang, H., Garimella, S. V., Murthy, J. Y. (2007). Characteristics of an evaporating thin film in a microchannel, *International Journal of Heat and Mass Transfer*, Vol. 50, pp. 3933-3942.

Wang, H., Rose, J. W. (2004). Effect of interphase matter transfer on condensation on low-finned tubes: a theoretical investigation, *International Journal of Heat and Mass Transfer,* Vol. 47, pp. 179-184.

Wang, H. S., Rose, J. W. (2006). Film condensation in horizontal microchannels: effect of channel shape, *International Journal of Thermal Sciences*, Vol. 45, pp. 1205-1212.
Wang, H. S., Rose, J. W. (2011). Theory of heat transfer during condensation in microchannels, *International Journal of Heat and Mass Transfer*, Vol. 54, pp. 2525-2534.
Wang, W. W. W., Radcliff, T. D., Christensen, R. N. (2002). A condensation heat transfer correlation for millimeter-scale tubing with flow regime transition, *Experimental Thermal and Fluid Science,* Vol. 26, pp. 473-485.